

FULL PAPER

REVIEW

SHORT COMMUNICATION

MULTIANALYTICAL CHARACTERISATION OF A VARIETY OF ULTRAMARINE PIGMENTS

V. DESNICA^{1*}, K. FURIĆ² AND M. SCHREINER^{1,3}

1. Institute of Sciences and
Technology in Art, Academy of
Fine Arts, Schillerplatz 3, 1010
Vienna, Austria

2. R. Bošković Institute,
Bijenicka cesta 54, 10002
Zagreb, Croatia

3. Institute of Chemical
Technologies and Analytics,
Analytical Chemistry Division,
Vienna University of
Technology, Getreidemarkt
9/164, 1060 Vienna, Austria

Corresponding author:

vladan.desnica@fch.akbild.ac.at

Abstract

Eleven different synthetic ultramarine pigments of a set of more than 1300 pigments at the Academy of Fine Arts in Vienna were chosen for a detailed study and comparative analysis. A thorough investigation was done by x-ray fluorescence analysis, x-ray diffractometry, Raman and infrared spectroscopy as well as colourimetry. The S_3^-/S_2^- ratio responsible for the hue of the pure ultramarine pigments as well as other compounds influencing the final hue of the colourant were precisely determined for each sample. A correlation between the relative concentration of the yellow chromophore, S_2^- , and the hue of the pigment has been established and the correlation between the colour saturation of the pigment and its hue was determined.

1. Introduction

Ultramarine has been for centuries one of the most highly prized pigments of all traditional artists' materials due to its durability, excellent colour, and its intrinsic value. It is made from the mineral lapis lazuli and although archaeological evidence shows that this mineral was used as a semi-precious stone and decorative building stone from early Egyptian times, the earliest occurrence of lapis lazuli used as a painting was in sixth- and seventh-century AD wall paintings in cave temples at Bamiyan in Afghanistan, not far from the most famous source of the mineral¹. In Europe, the pigment probably found its most extensive use in the fourteenth to mid-fifteenth centuries, particularly in illuminated manuscripts and in Italian panel paintings. Because of its high quality and most intense blue colour, ultramarine can often be seen to have been reserved for the robes of Christ and the Virgin. In the late sixteenth and the seventeenth century, it has been noted that there was a shortage of the other most valuable blue pigment, azurite, which must have resulted in increased demand for that already costly ultramarine, thus making it even more precious and expensive. Since the price of this extraordinary pigment was sometimes even higher than that of gold, the motivation for producing a synthetic version accelerated the quest for a more favourably-priced substitute and the first synthetic manu-

received: 17/03/2004

accepted: 24/06/2004

key words:

ultramarine, pigment, XRF,
XRD, Raman, FTIR

facturing of the ultramarine pigment succeeded in 1828¹. Because of their almost ten times lower price, they are being widely used in nearly all of the art works today, even though some critics claim they are less pure and less permanent than the pigment obtained from lapis lazuli².

The mineral lapis lazuli, from which the pigment is made, is a complex rock mixture¹. Fundamentally it is a mineralized limestone containing grains of the blue cubic mineral called lazurite with an approximate compositional formula $[(\text{Na},\text{Ca})_8(\text{Al},\text{Si})_{12}\text{O}_{24}(\text{S},\text{SO}_4)]$, which is the essential constituent of the pigment and primarily responsible for the intense blue colour of ultramarine. Chemically, it is one of the most complex of all the mineral pigments and it was traditionally obtained following a complicated method of selective extraction of the blue particles. In addition, lapis lazuli also contains other blue coloured minerals such as hauyne $[(\text{Na},\text{Ca})_{4-8}\text{Al}_6\text{Si}_6\text{O}_{24}(\text{SO}_4)_{1-2}]$, sodalite $[\text{Na}_8(\text{Al}_6\text{Si}_6\text{O}_{24})\text{Cl}_2]$ and noselite $[\text{Na}_8\text{Al}_6\text{Si}_6\text{O}_{24}(\text{SO}_4)]$, as well as mineral impurities like calcite (CaCO_3), pyrite (FeS_2), diopside ($\text{CaMgSi}_2\text{O}_6$), sphene (CaTiSiO_4), zircon (ZrSiO_4) etc³.

Its colour can range from royal deep blue, over ultramarine green, to ultramarine violet (or red) depending on the modification to the preparative procedures and on the manufacturing process. The key species in ultramarine responsible for its characteristic hue are the radical anions S_3^- and S_2^- , with S_3^- being a blue and S_2^- a yellow chromophore⁴. These polysulfide anions are occluded in an aluminosilicate matrix, which is comprised of vertex sharing Al/SiO_4 tetrahedra forming the sodalite cage (Figure 1)⁵. Each cage contains up to four cations and the centrally placed polysulfide.



Figure 1: Schematic view of the sodalite structure, the basic cage and the connection pattern. Full and open circles refer to Al, Si and oxygen, respectively.



Figure 2: The examined powderous ultramarine pigments in their original glass tubes and support, as part of the wide pigment database consisting of more than 1300 organic and inorganic pigments.

In the pigment collection of the Institute of Sciences and Technology in Art, Academy of Fine Arts in Vienna, Austria, 29 different types of ultramarine are present. Eleven of those samples were stored in similar glass tubes with similar labels, therefore presumably produced by the same company, and probably using the same technique (Figure 2). The exact date of the pigments is unknown but it can be assumed that they were produced at the end of the 19th beginning of the 20th century, as most of the pigments in the collection containing more than 1300 samples of various pigments and dyes originate from that period. Therefore, it was interesting to study how those particular ultramarine pigments differ regarding their elemental and chemical composition.

Investigations were carried out in order to determine if the reasons for the colour diversity of the samples are added materials, different S_3^- to S_2^- ratios or a combination of both. The sample numbers of the investigated pigments in this work correspond to the inventory numbers of pigments in the collection.

Five different analytical techniques, two x-ray methods – energy dispersive x-ray fluorescence (EDXRF) and powder x-ray diffraction (XRD) and three optical methods – colourimetry, Raman and Fourier transform infrared spectroscopy (FTIR) – were used. XRD, Raman and FTIR spectroscopy are specific to the compound, whereas XRF is specific to the elements present in the sample.

2. Experimental

2.1 Colourimetry

Colourimetry was implemented in order to characterize and organize the pigments according to their colours as well as to correlate colours of the examined pigments with different elemental and chemical composition. Colourimetry is a technique which could distinguish the colouring of the samples by using an objective and reproducible method with comprehensible parameters. It is based on the spectrum of the visible light and on the fact that each colour can be attributed to accurately defined wavelengths. Consequently, it can be arranged and systematically processed using various structuring systems. The CIELAB colour space system (Commission Internationale de l'Eclairage)⁶ was the system used to characterize each ultramarine pigment, applying the L^* , C^* , and h^* colourimetric parameters. These are the cylindrical coordinates of the CIELAB colour space and denote lightness, saturation, and hue, respectively. The lightness gives the ability of the sample to reflect or to absorb a fraction of the incident light ($L^* = 100$ for a white sample, $L^* = 0$ for a black sample). The saturation characterizes

a degree of the chromatic component contained in the colour. It ranges from 0 to 100, where 0 has the meaning that there are only achromatic components (grey colours) present in the sample, 100 refers to pure chromatic components. It can be interpreted as colour intensity. Parameter h^* represents the hue angle ($h^* = 0^\circ$ for a red colour, $h^* = 90^\circ$ for a yellow colour, $h^* = 180^\circ$ for a green colour and $h^* = 270^\circ$ for a blue colour).

The colourimetric measurements were carried out with a Gretac SPM 50 Spectrophotometer. The pigment samples were spread into round pellets with a thickness of ca. 1 mm and the remission spectrum was measured. These reflectance data of the samples were used to determine the colourimetric parameters L^* , C^* , and h^* .

2.2 X-Ray Fluorescence Analysis

The EDXRF measurements were carried out with a Tracor X-ray "Spectrace 5000" energy dispersive x-ray fluorescence analyzer. This instrument employs a low power x-ray tube (less than 50 W) with a Rh anode and a liquid nitrogen cooled Si(Li) detector. Acceleration voltages of 8, 30, and 50 kV were applied for the excitation of the samples. The 8 kV measurements were performed in vacuum, the 30 and 50 kV analyses were carried out in air.

2.3 Powder X-ray Diffraction

In order to identify the crystalline phases of the pigments, the crystalline compounds were examined by the means of XRD using a Siemens D5000 x-ray powder diffractometer. A θ - θ -goniometer (diameter 401 mm) equipped with a Cu-tube with the excitation conditions of 40 mA and 40 kV was available therefore. Each specimen was irradiated for 10 h and the obtained diffraction pattern was subsequently analyzed using the EVA MFC Application Software[®]. The patterns obtained were compared with the unique Powder Diffraction File (PDF), and the chemical composition of the pigments was determined (there are about 120,000 patterns in the current complete database). PDF[®] is a registered trademark of the JCPDS – International Center for Diffraction Data (ICDD) database. The high advantage of XRD is its accuracy in characterizing and identifying a specific compound as each crystalline phase has its well defined diffraction pattern, which acts as a finger-print of the crystalline substance. From the position, intensity and HWHM values of the diffraction maxima the unit cell, the crystal structure, and the size of the crystallite, respectively, can be defined. Samples of the same chemical composition but of different forms (crystalline modifications) can also be differentiated, like in the case of CaCO_3 , which can occur as calcite

(e.g. as an addition in the ultramarine pigments), as aragonite, or as vaterite.

2.4 Infrared Spectroscopy

Fourier transform infrared spectra of the ultramarine samples were recorded at room temperature using a Perkin Elmer spectrometer, model 2000. It is equipped with a voltage-stabilized, air-cooled, tungsten halogen source with a quartz envelope and a MIRFR-DTGS (Mid Infrared Fast Recovery Deuterated TriGlycine Sulfate) detector. Even though the liquid nitrogen cooled MCT (Mercury Cadmium Telluride) detectors are faster and more sensitive, the DTGS detector with a wider wavenumber range (optimum range $7800\text{--}370\text{ cm}^{-1}$) was chosen, so that the presence of the blue chromophores in the samples - with the vibration band at around 580 cm^{-1} could be determined, if present. The system used is coupled with a personal computer which is loaded with the Spectrum v3.02[®] software for fast processing of the recorded signals. Samples were carefully milled and mixed together with KBr powder using an agate set of tools and then pressed into standard pellet forms (0.5-0.7 mm thickness). Since KBr powder is transparent to the infrared radiation (i.e. the spectrum will not be affected and/or altered), it is particularly useful as a binding medium in such investigations, when only small amounts of sample material is available.

2.5 Raman Spectroscopy

The Raman spectrum, a result of the Raman frequency shift, yields direct information of the molecular vibrational frequencies of a sample. This can be used to identify the molecular composition of the molecules in the sample by comparing with the spectra of standards.

Argon-ion laser Coherent, model Innova 100-15, was used for excitation of the Raman spectra. The beam of 514.4 nm wavelength was filtered by a double premonochromator (elimination of spurious plasma lines) and attended with an interface filter to keep the beam power of 100 mW at the sample place in order to minimize the risk of thermal decomposition of the samples at the beam focus. Spectra were recorded in backscattering geometry by a computerized DILOR triple monochromator model Z24 at room temperature, improved with a cooled C31034 RCA photomultiplier. Samples were prepared from pigments in a powder form, which were pressed together in small pellets of 4 mm in diameter and 0.5-1 mm thickness. A technique of line illumination was used to prevent possible overheating of such sensitive materials. The measurements were performed at the R. Bošković Institute in Zagreb, Croatia.

3. Results and Discussion

3.1 Colourimetry

A blue ultramarine pigment without any added compounds or impurities contains mostly the S_3^- blue chromophore with a small amount of the S_2^- yellow chromophore, whereas in the green ultramarine pigments the ratio of the yellow chromophore to the blue one is much higher⁷. Some of the ultramarine samples in the collection of the Academy of Fine Arts show a deep blue colour, others a green colour, which can be seen in Figure 2.

The correlation of the visual perception of the pigment hue and the measured h^* values defined the value $h^* = 270$ as the limit between the deep blue pigments ($h^* \geq 270$) and the greenish blue pigments ($h^* \leq 270$). From those measurements as well as from the results of previous studies⁷ it could be expected that an increase of the relative concentration of the yellow chromophore S_2^- would yield a decrease of the h^* values. Consequently, the pigment would appear more greenish. This tendency is clearly seen in Figure 3.

Additionally, in the same figure, the deviation for many samples from the expected linearly decreasing h^* values with an increase of a relative S_2^- concentration could be noticed (correlation coefficient, $R = 0.85$, standard deviation, S.D. = 0.025). This suggests the presence of other components, which are also responsible for the final hue of the pigments.

It is interesting to note that the hue h^* and the saturation C^* of the pigments seem highly correlated, as seen in Figure 4. With the increase of the hue parameter h^* (implying the increase of the S_3^-/S_2^- concentration ratio, which was determined from the Raman measurements), the saturation values are increased as well, hence, the

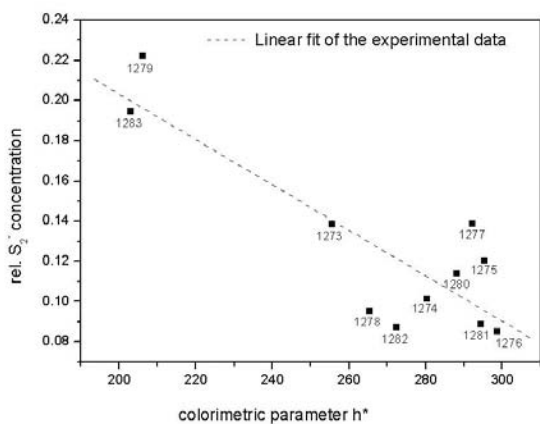


Figure 3: Concentration of S_2^- (relative to the concentration of S_3^-) as determined from the Raman measurements plotted versus the colourimetric parameter h^* , for the various ultramarine pigments investigated.

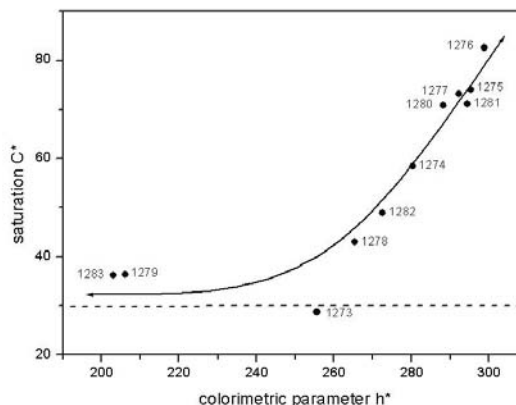


Figure 4: Saturation C^* of the various ultramarine pigments versus their colourimetric parameter h^* .

bluer the sample, the more saturated it is. Therefore, the difference observed between the saturation of the blue and green pigments is an indication that mostly the blue chromophore, S_3^- , is responsible for the saturation, and consequently for the intensity of the colour. It should be noted that for the two samples no. 1279 and 1283 with the greatest fraction of the yellow chromophore, the lowest saturation limit has been reached (dotted line) and no further decrease of the C^* values can be observed. This limit corresponds to the previously defined limit between the blue and greenish-blue pigment, set to the hue value of 270.

3.2 EDXRF and XRD

Energy dispersive x-ray fluorescence analysis (EDXRF) yielded a complete and accurate determination of the elements with an atomic number ≥ 11 in the samples. Beside the elements contributed to pure synthetic ultramarine (Na, Al, Si, S) a number of other elements from admixtures,

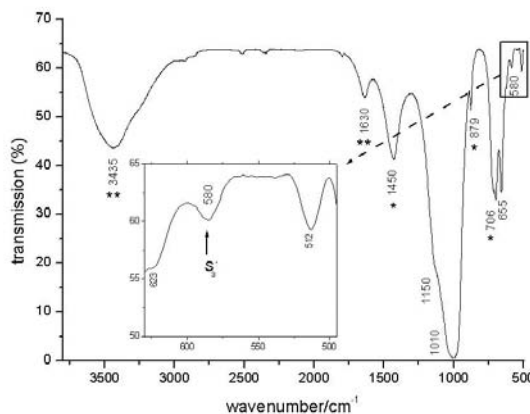


Figure 5: Fourier transform infrared spectrum of the pigment no. 1282 showing the absorption bands for ultramarine (the bands marked with one and two asterisks are attributed to calcite and water due to humidity, respectively). The inserted spectrum shows the 800-500 cm^{-1} interval. ν_3 vibration band at 580 cm^{-1} belonging to the ion S_3^- , confirming the presence of the blue chromophore responsible in the first place for the intensive blue hue of the ultramarine pigments is clearly visible.

Sample No.	1273	1274	1275	1276	1277	1278	1279	1280	1281	1282	1283
Ultramarine	+	+	+	+	+	+	+	+	+	+	+
Calcite	+	+	+	-	-	+	-	+	+	+	+
Anatase	+	-	-	-	-	+	-	-	-	+	-

Table 1: List of crystalline phases determined by XRD in the various samples.

Sample No.	1273	1274	1275	1276	1277	1278	1279	1280	1281	1282	1283
Raman	Um, TiO ₂	Um	Um	Um	Um	Um, TiO ₂	Um	Um	Um	Um, TiO ₂	Um
IR	Um Calcite	Um Calcite	Um Calcite	Um	Um	Um Calcite	Um	Um	Um Calcite	Um Calcite	Um Calcite

Table 2: List of components determined in the samples by Raman and IR spectrometry (Um = ultramarine, TiO₂ = anatase)

impurities etc. were determined: Fe, Ti, Sr, Ba, Zn, Ga, As, Ca, Zr, Pb Cr, Cu, Zn, K, Mn.

Although all the ultramarine samples are synthetic pigments, elements such as Fe, Ti, Zn or even Br, which should not be present in a pure synthetic ultramarine, could be determined. As ultramarine is synthesized from china clay from a clay pit, the probable reason for the existence of these elements is that Fe, Ti and Zn are present in micas which are in china clay. Therefore, it must be assumed that the samples contain various admixtures and also impurities resulting from the manufacturing process. Consequently, it must be concluded already from the EDXRF results that ultramarine, richer in its elemental composition than the chemical compounds lazurite, hauyne, or sodalite request, does not mean necessarily that the material is of natural origin, as suggested in the literature³. The high amount of Ti and Ca in some of the samples could be clearly understood from the XRD results, whereas the presence of Br in the sample no. 1277 could not be explained so far.

Powder x-ray diffraction (XRD) of the ultramarine pigments showed unambiguously that the main colour component is the blue pigment sodium-aluminum-silicate-sulfide (Na₇Al₆Si₆O₂₄S₃). In the samples no. 1273, 1278 and 1282 anatase (a modification of titanium dioxide, TiO₂) was also verified, which could be proved by Raman spectroscopy. Additionally, calcite could be identified in the samples no. 1273, 1274, 1275, 1278, 1280, 1281, 1282 and 1283, as summarized in Table 1.

It is important to note that the strongest diffraction maxima of the natural ultramarine components lazurite, noselite, and hauyne have shown strong similarities regarding their d-values. Therefore, it is very difficult to differentiate between these three components. This points to the fact that all those minerals have similar crystal structures and can only be distinguished by comparative analysis of additional different methods, such as FTIR or Raman spectroscopy³.

3.3 FTIR Spectroscopy

The absorption bands of the eleven pigments analyzed with Fourier transform infrared (FTIR) spectroscopy confirmed the assumption that the pigments are ultramarine blue. As shown in Figure 5, the characteristic ultramarine framework absorption bands of the sodalite structure are dominating with a wide band centered around 1010 cm⁻¹ in the Si-O stretching region of the aluminosilicate matrix, which has also a recognizable asymmetric shape from a shoulder near 1150 cm⁻¹.⁸

In addition to the Si-O vibrations, aluminosilicates [(Al₆Si₆)O₂₄] exhibit Al-O vibrations which are clearly visible in the 750-650 cm⁻¹ region⁹. Some additional absorption bands below 600 cm⁻¹ are bending vibrations of Si-O.¹⁰ Additionally, the n₃ vibration band of S₃⁻ at about 580 cm⁻¹ is also well established⁸, confirming the presence of the blue chromophore.

The white colourant titanium dioxide (TiO₂) used in some of the pigments (e.g. samples no. 1273, 1278 and 1282) to change their hues, is not Mid-IR active because of its stretched bond and, therefore, can not be observed using mid-infrared spectroscopy. Therefore, the IR spectrum of the mixture may not represent the total composition of the material. For example, titanium dioxide, as said before, does not have any absorption bands in the mid-IR region, but a commercial product containing fillers, such as clay or barium sulphate, would produce a characteristic spectrum. The recorded spectrum would in this case identify the fillers and neglect TiO₂.¹⁰

The presence of calcite (CaCO₃) was also confirmed in most of the samples with the IR absorption bands at 706, 879 and 1450 cm⁻¹.⁹ However, this could not be proved for four (samples no. 1276, 1277, 1279, 1280) of the eleven ultramarine samples examined due to rather weak absorption bands typical for calcite and a strong coincidence of the most characteristic calcite peak at 879 cm⁻¹ with the broad ultramarine band centred around 1020 cm⁻¹. FTIR results of the

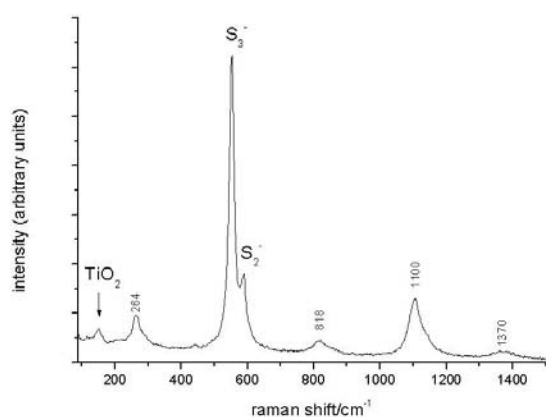


Figure 6: Raman spectrum of the pigment no. 1273, where a TiO_2 peak at 145 cm^{-1} is clearly visible. The S_3^- and S_2^- peaks at 550 and 585 cm^{-1} , respectively, and peaks at 264 , 818 , 1100 , and 1370 cm^{-1} identified as ultramarine peaks are evident as well.

investigated pigments are summarized in Table 2.

The broad band, which appeared in each spectrum around 1630 cm^{-1} , is associated with deformation vibrations $\delta(\text{OH})$ and together with $\nu(\text{OH})$ stretching frequencies at 3435 cm^{-1} the presence of water in the samples can be concluded due to humidity^{11,12}. This assumption could be proved by a subsequent measurement of the dry samples (dried for 24 h at $110\text{ }^\circ\text{C}$) under additional purging of the sample chamber of the FTIR instrument with dry air. The FTIR spectra obtained showed that the relative intensities of the bands characteristic for water decreased dramatically.

Weak absorption bands at 1340 , 667 and 2350 cm^{-1} denote the normal modes of vibrations ν_1 , ν_2 , and ν_3 of CO_2 , respectively⁹, even though the atmospheric correction routine was implemented, and are therefore assumed to be disregarded. When CO_2 correction is being carried out the software uses a single reference spectrum derived from high resolution data to model the line shape and then finds the current real instrument parameters by least squares fitting to the measured spectrum¹³.

3.4 Raman Spectroscopy

The Raman spectra confirmed the results obtained by FTIR spectroscopy and proved once again that the samples are indeed ultramarine based. A characteristic spectrum referring to the sample no. 1273 is shown in Figure 6. The distinctive peaks of ultramarine¹³ are detected at 255 , 550 , 585 , 807 , 1100 and 1360 cm^{-1} .

The two strongest peaks at 550 and 585 cm^{-1} correspond to Raman shifts for S_3^- (blue chromophore) and S_2^- ions (yellow chromophore), respectively⁶, whereas the 550 cm^{-1} peak is the symmetric stretch of the radical ion matrix isolated in the alumino-silicate lattice¹⁴. Previous works have established that both are present in ultramarine blue⁴, although the S_3^- is in by far greater amount and is thus primarily responsible for the blue colour of the pigment.

For pure ultramarine pigments the ratio $\text{S}_3^-/\text{S}_2^-$ defines the hue of the pigment, from deep blue (mostly S_3^-) to light green-yellowish blue (great amount of S_2^- present as well). S_3^- and S_2^- related peaks in the Raman spectrum were fitted with Lorentzian functions after background subtraction. The relative $\text{S}_3^-/\text{S}_2^-$ area ratios for each sample are given in Table 3.

It is interesting to see that the percentages of S_2^- to S_3^- ion range from only 8.87 % in the sample no. 1281 to even 34.5 % in the sample no. 1273. These results suggest already great differences in the hue of the pigments ranging from deep blue to greenish light blue. The colourimetric measurements carried out in order to confirm this assumption showed, however, that the hues of many pigments deviated from expected values implying that there are other admixtures and components responsible for a change of the basic pigment hue.

A distinctive peak at 145 cm^{-1} indicates the presence of anatase, a modification of titanium dioxide (TiO_2),¹⁵ as obtained by XRD. Because of their high refraction index (anatase 2.55, rutile 2.75) white TiO_2 pigments have an extraordinary illuminating and cover capability and are therefore often being added to brighten the coloured pigments¹⁶. Anatase occurs in nature as a mineral, but always contains some inclusions, which darken its bright colour. It was in 1923, when a process could be developed for manufacturing pure white anatase. This oxide (along with rutile) has thus been proved to be exceptionally good for dating artists' materials and distinguishing between old (produced before 1923) and modern colourants¹⁵. In our case the examined ultramarine samples could not have been produced before 1923.

The presence of calcite (CaCO_3), probably used to brighten the pigments as well, which was already confirmed in most of the samples by XRD and IR spectroscopy, could not be explicitly veri-

Sample No.	1273	1274	1275	1276	1277	1278	1279	1280	1281	1282	1283
Area S3/S2	2.9	7.33	5.34	7.96	3.27	8.18	3.8	5.42	11.27	7.7	3.85
% S2 of S3	34.53	13.65	18.74	12.56	30.58	12.23	26.28	18.46	8.87	13	26

Table 3: The $\text{S}_3^-/\text{S}_2^-$ ratios calculated from the fitted Raman spectra as well as the percentage of S_2^- ion to S_3^- .

fied by Raman spectroscopy, because of the high coincidence between the strongest calcite peaks at 1087 and 283 cm^{-1} and the characteristic ultramarine spectrum¹⁵.

4. Conclusions

A detailed comparative analysis of eleven different synthetic ultramarine pigments has been performed using x-ray fluorescence, x-ray diffractometry, Raman and infrared spectroscopy as well as colourimetry. It has been shown that only the combination of all these methods enables to gather enough information for full differentiation of the samples, and to obtain a thorough characterization of each pigment. Although all eleven analyzed pigments were synthetic, the methods have shown that all of them beside pure synthetic ultramarine, contain other elements and other colourants as well. Therefore, the purity vs. variety and complexity of compounds and elements found in examined pigment should not be taken as an important criterion to differentiate synthetic from natural ultramarine pigments.

An expected negative general trend between the hue of the pigments and the relative concentrations of the S_2^- and S_3^- ions (yellow and blue chromophores) has been observed. However, the correlation was quite weak indicating that, besides the modifications of the $\text{S}_3^-/\text{S}_2^-$ ratio, the hue was altered through intentional addition of some other colourants, like calcite or anatase. The presence of synthetic anatase in some samples indicate that these ultramarine pigments could not have been older than the year 1923.

Furthermore, the increase of the colourimetric parameter defining the hue of a pigment, h^* , was found to be related to the increase of saturation of the pigment as well, thus showing that mostly the blue chromophore, S_3^- , is responsible for the saturation, and consequently for the intensity of the colour.

References

1. J. Plesters, *Ultramarine blue, natural and artificial*, in: A. Roy, ed., *Artists' Pigments*, vol. 2, Oxford University Press, New York, 1993, 39-56.
2. R. D. Harley, *Artists' Pigments c. 1600-1835*, Butterworths, London, 1970, 55-56.
3. S. Bruni, F. Cariati, F. Casadio, L. Toniolo, *Spectrochemical characterization by micro-FTIR spectroscopy of blue pigments in different polychrome works of art*, *Vib. Spectrosc.*, 1999, **20**, 15-25.
4. R. J. H. Clark, T. J. Dines, M. Kurmoo, *On the nature of the sulfur chromophores in ultramarine blue, green, violet, and pink and of the selenium chromophore in ultramarine selenium: characterization of radical anions by electronic and resonance Raman spectroscopy and the determination of their excited-state geometries*, *Inorg. Chem.*, 1983, **22**, 2766-2772.
5. D. Reinen, G.-G. Lindner, *The nature of the chalcogen colour centers in ultramarine-type solids*, *Chem. Soc. Rev.*, 1999, **28**, 75-84.
6. N. Gobeltz, A. Demortier, J. P. Lelieur, C. Duhayon,

Encapsulation of the chromophores into the sodalite structure during the synthesis of the blue ultramarine pigment, *J. Chem. Soc., Faraday Trans.*, 1998, **94**, 2257-2260.

7. N. Gobeltz, A. Demortier, J. P. Lelieur, C. Duhayon, *Correlation between EPR, Raman and colorimetric characteristics of the blue ultramarine pigments*, *J. Chem. Soc., Faraday Trans.*, 1998, **94**, 677-681.

8. S. Bruni, F. Cariati, F. Casadio, L. Toniolo, *Identification of pigments on a XV century illuminated parchment by Raman and FTIR microspectroscopies*, *Spectrochim. Acta, Part A*, 1999, **55**, 1371-1377.

9. K. Nakamoto, *Infrared and Raman Spectra of Inorganic and Coordination Compounds*, Part A, 5th edition, Wiley, New York, 1990, 153-175.

10. M. R. Derrick, D. Stulik, J. M. Landry, *Scientific Tools for Conservation – Infrared Spectroscopy in Conservation Science*, J. Paul Getty Trust, Los Angeles, 1999, 113-120.

11. M. T. Domenech Carbo, F. Bosch Reig, J. V. Gimeno Adelantado, V. Periz Martinez, *Fourier transform infrared spectroscopy and the analytical study of works of art for purposes of diagnosis and conservation*, *Anal. Chim. Acta*, 1996, **330**, 207-215.

12. K. Nakamoto, *Infrared and Raman Spectra of Inorganic and Coordination Compounds*, Part B, 5th edition, Wiley, New York, 1990, 109.

13. L. I. McCann, K. Trentelman, T. Possley, B. Golding, *Corrosion of ancient Chinese bronze money trees studied by Raman microscopy*, *J. Raman Spectrosc.* 1999, **30**, 121-132.

14. L. Burgio, D. A. Ciomartan, R. J. H. Clark, *Pigment identification on medieval manuscripts, paintings and other artefacts by Raman microscopy: applications to the study of three German manuscripts*, *J. Mol. Struct.*, 1997, **405**, 1-11.

15. L. Burgio, R. J. H. Clark, *Library of FT-Raman spectra of pigments, minerals, pigment media and varnishes, and supplement to existing library of Raman spectra of pigments with visible excitation*, *Spectrochim. Acta, Part A*, 2001, **57**, 1491-1521.

16. *Römp Chemie Lexikon v1.0*, Georg Thieme Verlag, Stuttgart, New York, 1995.